Fault Identification of Ball Bearings using Fast Walsh Hadamard Transform, LASSO Feature Selection, and Random Forest Classifier

V. Dave
Department of Mechanical Engineering
School of Technology
Pandit Deendayal Energy University
Gujarat – 382007
India

H. Thakker
Department of Mechanical Engineering
Columbia University
New York – 10027
United States

V. Vakharia
Assistant Professor
Department of Mechanical Engineering
School of Technology
Pandit Deendayal Energy University
Gujarat – 382007
India

To reveal the machinery health condition, time-frequency analysis is an effective tool when signals are non-stationary. To identify bearing faults, numerous techniques have been proposed by various researchers. However, little research focused on image processing-based texture feature extraction for the identification of faults. The time-frequency image contains many sensitive fault information regarding bearing conditions, which can be extracted in the form of features. Therefore, in this paperwork, a methodology is proposed based on Fast Walsh Hadamard Transform (FWHT) time-frequency spectrogram, gray level co-occurrence matrix (GLCM), and machine learning techniques. A feature vector is constructed which consists of one dimension and two-dimension features extracted from Fast Walsh Hadamard Transform coefficients. To identify the fault conditions, LASSO-based feature ranking is applied to determine the suitable features. Finally, classifiers like Support vector machine (SVM), Random forest, and K-nearest neighbors (KNN) are evaluated for identifying bearing faults. Training, Testing, five-fold cross-validation performed on fusion feature vector. Results indicate that ranked fusion features are effective to diagnose bearing faults with good accuracy.

Keywords: Bearing Faults, FWHT, GLCM, LASSO, Random Forest

1. INTRODUCTION

Rolling bearings are a key component used in industrial machinery. It is observed that failure of bearing leads to the breakdown of machinery and production losses, therefore the diagnosis of bearing faults is essential. In the last few decades, researchers identifies various techniques to diagnose bearing faults in running or stationary conditions. To avoid unexpected breakdowns and catastrophic failure of machinery various methods are used, like wear debris analysis, acoustic emission, vibration, thermal infrared, etc. Vibration-based fault diagnosis emerged as the most effective technique to diagnose faults, due to its effectiveness to monitor the conditions of machinery in a running state[1-6]. However, it is a challenging task to deal with the vibration signals which continuously change with time. Features computed from the time and frequency signals were examined in detail to diagnose multiple fault conditions in bearings[7]. When Fast Fourier Transform (FFT) is applied to detect an incipient fault, the harmonic characteristic frequency is difficult to detect due to the inherent noise. Therefore it is difficult to identify the characteristic frequency by direct spectrum analysis[8]. To analyze the non-stationery signal, the time-frequency analysis method has been successfully applied and found to be effective, due to the generation of both time and frequency information of signal simultaneously. Short-time Fourier transform (STFT) [9], Wavelet Transform [10], Empirical mode decomposition (EMD) are widely used and successfully applied to diagnose the faults[11]. However, each method has its pros and cons depending upon the nature of the signal and the effectiveness of techniques applied to diagnose faults. The drawback of STFT is fixed window size, which is not suitable to get good time resolution at higher frequencies and good frequency resolutions at lower frequencies simultaneously. On the other hand, Wavelet transforms (WT) emerge as an effective time-frequency signal processing technique to investigate and diagnose bearing faults. However, the selection of base wavelets is still a challenging task [12]. Huang et al.[13], proposed Empirical mode decomposition (EMD) as an adaptive signal time-frequency method for the analysis of nonlinear and non-stationary signals. Authors successfully applied EMD and its variants for fault diagnosis but it has a certain disadvantage too. Mode mixing is the biggest disadvantage of EMD, followed by a wide frequency band obtains from intrinsic mode functions. Recently the effectiveness of Walsh Hadamard transforms (WHT), to diagnose faults has been reported by various authors [14-15]. WHT is a generalized class of Fourier transform and its characteristics are, it is a non-sinusoidal, orthogonal transformation technique that depends upon a set of basis or Walsh function. The size of the matrix is square waves with values of +1 or −1. Compared to the FFT, the fast Walsh-Hadamard transform (FWHT) requires less storage space and only uses real additions and subtractions, while the FFT

Received: May 2021, Accepted: December 2021
Correspondence to: Dr Vinay Vakharia, Department of Mechanical Engineering, School of Technology, Pandit Deendayal Energy University, India.
Email:vinay.vakharia@sot.pdpu.ac.in
Doi: 10.5937/fme2201202D

needs intricate details [16]. Because of its unique advantage of representing signals with sharp discontinues, it can be strongly applied in the field of fault diagnosis, signal processing, and image processing [12-17].

In bearing, defects are classified as Ball defect (BD), Outer race defect (ORD), Inner race defect (IRD), cage defect, etc. Due to the operating conditions, geometry, and friction at surfaces, different faults are developed. When these fault characteristics are represented with either scalogram or spectrogram, then extraction of texture features plays an important role. Recently various authors conducted experimental studies to explore the suitability of texture features for bearing fault classifications. Texture analysis methods such as gray-level co-occurrence matrix (GLCM) [18], local binary patterns (LBP) have been applied in tool condition monitoring[19], surface roughness determination [20] , face recognition [21], EEG classification [22] are some of the application areas where texture analysis is given significant results. GLCM which is proposed by Haralick et al. [18] is considered a powerful technique to analyze the texture features computed from the time-frequency spectrogram. GLCM is applied in various fields of engineering and medical science [23]. Chen et al. [24] proposed fault diagnosis methods relevant to texture features computation from adaptive optimal kernel time-frequency spectrogram and uniform local binary patterns. A detailed experimental study has been carried out and the results reveal the usefulness of the methodology. In another study, texture features-based fault diagnosis methods using S-Transform and GLCM were proposed by Zhao et al. [25]. Results indicate the advantage of extracted texture features to identify various bearing faults using Support Vector Machine (SVM). Potential benefits of feature selection methods were explored to enhance the fault diagnosis accuracy. The aim is to identify significant features and discard irrelevant features, to form a new subset of feature vector which is less in dimension. Chi-Square feature ranking method utilized by Vinay et al. [26] to diagnose bearings faults using Random Forest and the diagnosis accuracy is found to be satisfactory. A ten-fold cross-validation procedure was applied to get statistically unbiased results. Results reveal improvement in fault diagnosis accuracy when a ranked feature vector was used. Mutual Information [27], Fisher score [28], Malhanobis distance [29] are the techniques used for feature ranking. In the present study, a methodology is proposed to extract the 1-D and 2-D (time-frequency images) statistical features from Fast Walsh Hadamard Transform. LASSO feature ranking techniques have been applied to select the most informative features and a modified feature set was constructed. Case Western Reserve University (CWRU) bearing data set was used to conduct the experimental study. The combination of ranked feature vectors and classifiers is applied to get the maximum fault diagnosis accuracy. Considering the fewer variations in rotational speed of shaft, minimal fault size, the ranked feature set is divided into training and testing sets. To achieve statistically unbiased results k-fold cross-validation procedure is applied. The results obtained reveal the utility of the proposed method. The major advantage of the methodology is to utilize a novel feature set which consists of features extracted from vibration signals (1-D) and texture features (2-D) to diagnose the bearing faults. The paper is organized as follows: Brief descriptions of FWHT and GLCM is presented in Section 2 and 3. In Section 4 machine learning techniques are discussed in brief, followed by the LASSO feature selection technique in section 5. The experimental procedure and results are highlighted in sections 6 and 7. Finally, the conclusion is highlighted in section 8. Figure 1shows the methodology used to carry out the study.

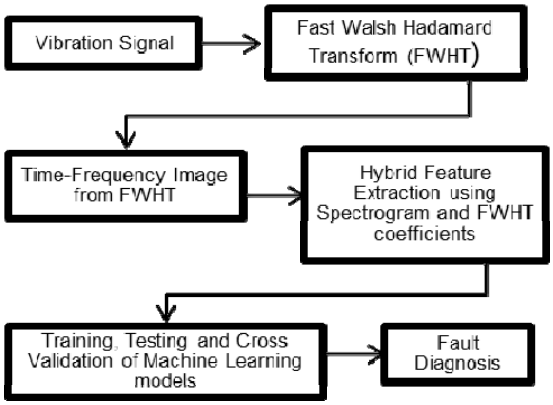

Figure 1. Flowchart for fault diagnosis methodology

2. FAST WALSH HADAMARD TRANSFORM (FWHT)

Fast Walsh-Hadamard transform can be applied in different fields of engineering like data compression, speech, and image processing. Due to its inherent characteristic of orthogonal transformation, a signal is decomposed into a rectangular waveform with only binary values of ± 1. This transformation has also been adopted as a low-complexity transform method for image processing. In this study, a fast version of WHT is used, as it doesn't require storage space and takes less computational time compared to Fast Fourier Transform (FFT). The Fast Walsh-Hadamard transform (FWHT) for a signal z(t) of length N can be given by:

$$y_n = \frac{1}{N}\sum_{j=0}^{N-1} z_j WL(n,j) \tag{1}$$

where j = 0, 1,…,N-1 and WL(n,j) are Walsh functions. The N number of elements is breakdown into two parts with N/ 2 number of elements after which they are combined to form FWHT [30].

3. GRAY LEVEL CO-OCCURRENCE MATRIX (GLCM)

GLCM represents a configuration of how frequently different blends of pixel brightness appear in an image. A GLCM matrix is a method to calculate the relationship of an image pixel. The picture is a component of two variables (x,y). Gray Level Co-Occurrence Matrix (GLCM) is a measurable technique for separating a textural include from a spectrogram image. The Gray-Co-Matrix function generates a gray-level co-occurrence matrix (GLCM) by computing how often a pixel with the intensity value i appears with a spatial connection to a pixel with the value j.To

illustrate this, Figure 2 shows how the Gray-Comatrix quantifies the values in a GLCM. In the output of GLCM, element (1,1) contains the value 2 because there are only two instances in the input image while two horizontally adjacent pixels have the values 1 and 1, respectively. GLCM (5, 4) contains the value 1 because there is only one instance where horizontally adjacent pixels have values 5 and 4. The process continues for scanning the images to other pixel pairs (x,y) and calculates values for other corresponding elements of the GLCM [31].

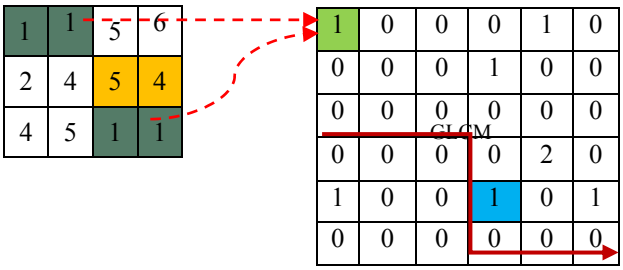

Figure 2. GLCM matrix

4. MACHINE LEARNING ALGORITHMS

4.1 Support Vector Machine

Due to its multiple disciplinary applications like EEG, condition monitoring, fault diagnosis, neuroscience, and many more, the support vector machine is the most preferable classifier[32]. It is one of the important machine learning algorithms. There are various types of kernels available i.e. linear, quadratic, cubic, Gaussian, etc. In this study, Radial Basis Function (RBF) kernel is considered. Kernel-based SVMs are implemented when data cannot be linearly separated by a hyperplane for classification[33].

4.2 K - Nearest Neighbor (KNN) Classifier

The KNN is a memory-based classifier, it uses a majority vote ofk neighbor's nearest distance to the instance which is in consideration. To calculate the distance between instances of various fault conditions, Euclidean distance is primarily used in feature space. The KNN performs pretty well in the scenarios where the decision boundaries are very irregular and where each class has several different subtypes [34-35]. It is considered an effective machine learning model for prediction and it's applied satisfactorily for various applications such as fault diagnosis, image classification, etc.

4.3 Random Forest (Ensemble Bagged Trees)

Ensemble learning provides an advantage over the conventional decision trees algorithm as it uses a combination of different models to mitigate the bias of a single model. The Random Forest algorithm which employs the ensemble of bagged trees works similarly, by taking decision trees of various depths and splits randomly and creating an ensemble of trees. Bootstrap Aggregation (Bagging) creates multiple sets for training from a single data set [36]. Another advantage of this method is that the performance of a single decision tree does not matter and thus the trees with greater depth and splits can be trained without worrying about the issues of higher variance and thus overfitting. The prediction about the class of example is made by taking a majority vote from the individual members of the model [37].

5. FEATURE SELECTION USING LASSO

LASSO (Least Absolute Shrinkage and Selection Operator) is useful for prediction as well as for feature selection. While applying ML, a feature vector is randomly split into training and testing of data, most often in the ratio 70:30.To avoid overfitting of data as well as to achieve a lesser variance with the tested data, regularization is carried out by computing a "penalty" parameter to the extracted coefficients [38].In general, regularization is of two types: L1 and L2. LASSO regression is based on the implementation of L1 regularization which is based on sparse models to compute fewer coefficients. The variables which are having a non-zero coefficient after the shrinking process is applied, are preferred as a relevant feature. LASSO is mathematically represented as:

$$\sum_{i=1}^{n}\left(y_i-\sum_j x_{ij}\beta_j\right)^2+\lambda\sum_{j=1}^{p}\left|\beta_j\right| \qquad (2)$$

where λ represents the magnitude of shrinkage. For feature selection, λ =0 indicates all features are considered, and λ = ∞ indicates no feature is selected. Finally, it increases the interpretability of the model is increased by eliminating unrelated variables which are less associated and, in turn, allows to reduce overfitting [39].

6. EXPERIMENTAL PROCEDURE

6.1 CWRU Dataset

To carry out the study, bearing data from the Case Western Reserve University (CWRU) with different speeds and bearing conditions are taken into account [41]. The drive end of the motor and dynamometer are joined with the help of a coupling device, and with the help of the accelerometer vibration signal is captured which is shown in Fig. 3. Signals are recorded from the drive side of the bearing with different conditions as (1) normal bearing (NB); (2) inner race fault (IR); (3) ball fault (BF); (4) outer race fault (OR) and variation in rpm of the shaft are 1730, 1750, 1772 and 1797 rpm respectively. Parameters of deep-groove ball bearing are listed in Table 1.

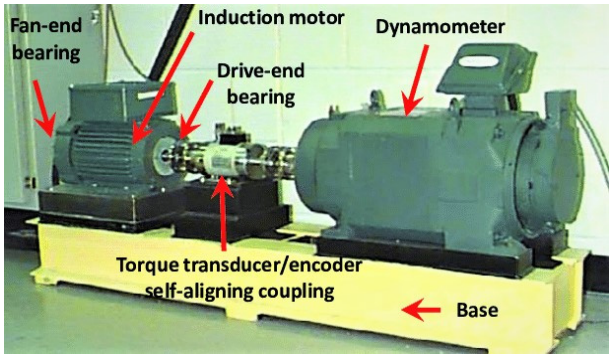

Figure 3. Bearing Test Rig (CWRU)

Table 1. Bearing Data

Sr.No.	Name	Value
1	Bearing type	6205 (SKF)
2	Outside run dia. (mm)	52
3	Inside run dia. (mm)	25
4	Ball dia. (mm)	7.94
5	Number of balls	9
6	Contact angle	α

6.2 Bearing Characteristic Frequency

The bearing consists of four components: the outer race, inner race, ball, and cage. The corresponding frequencies associated is given by [40] :

$$F_{IR} = \frac{n}{2} f_r \left(1 + \frac{d}{D}\cos\alpha\right) \quad (3)$$

$$F_{OR} = \frac{n}{2} f_r \left(1 - \frac{d}{D}\cos\alpha\right) \quad (4)$$

$$F_{Cage} = f_r \left(1 - \frac{d}{D}\cos\alpha\right) \quad (5)$$

$$F_{Ball} = \frac{f, D}{2d}\left(1 - \left(\frac{d}{D}\right)^2 \cos\alpha^2\right) \quad (6)$$

where f_r is the rotational frequency of inner race d , is ball diameter, D is pitch diameter, n is the number of balls, and $\alpha$is the contact angle. Fig.4 indicates the FFT plot of different bearing conditions like normal, inner race, outer race, and ball fault. We also observe that the frequency associated with it is reflected in the amplitude-frequency graph according to the above equations. Time response and FFT plot are shown in Fig. 4 (a-d) for normal bearing at 1750 rpm and maximum amplitude appears at varying compliance (VC) 85.22 Hz is shown, in Fig. 4 (a). For other fault conditions of bearing like inner race and outer race maximum peak is observed at 157.97 Hz and 104.52Hz respectively shown in Fig. 4 (b-c). Peak is observed at 143.7 Hz, for ball fault which is double the peak of ball spin frequency (BSF), as shown in Fig. 4 (d).

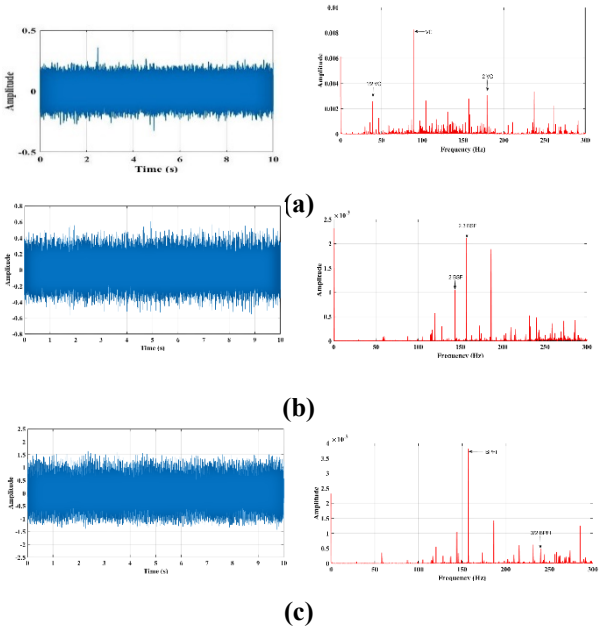

(a)

(b)

(c)

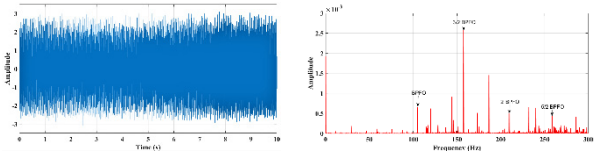

(d)

Figure 4: FFT plot at 1750 rpm category: (a) normal, (b) ball fault, (c) inner race fault (d) outer race fault.

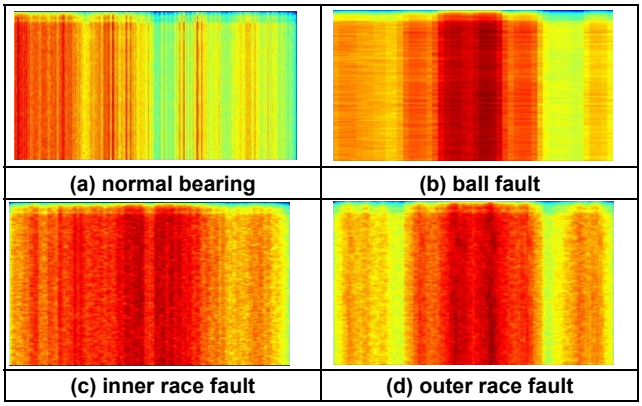

(a) normal bearing | **(b) ball fault**

(c) inner race fault | **(d) outer race fault**

Figure 5: Images for bearing at different fault sizes at 1750 rpm category: (a) normal, (b) ball fault, (c) inner race fault (d) outer race fault.

6.3 Fault Pattern Identification and Diagnosis Results

After acquiring the signals, the Fast Walsh Hadamard Transform is applied to extract the features from vibration signals. From the extracted coefficients, various spectrograms are generated and GLCM is applied to the spectrogram to extract the features. The feature vector is constructed of size 64 × 46 which is the combination of one dimensional and two-dimensional features. The spectrogram of various states of bearing is shown in Fig. 5. Each spectrogram shows the distinct characteristics of bearing conditions 1750 rpm. Fig. 5(a) shows the normal bearing condition at 1750 rpm. Likewise, Fig. 5(b) corresponds to the ball fault. Fig. 5(c-d) corresponding to inner fault defect and outer fault defect. We observed that color intensity and distribution of spectrogram are changing from healthy to the defective bearing. It is difficult to distinguish the fault directly from the images. Therefore, some relevant texture feature has to be extracted for different fault conditions. One dimension and two dimensions features are mentioned in Table 2. The range of variation of each feature is different as compared to other features. To overcome this, feature normalization is done to ensure all the features are on a similar scale. Z-score Normalization is given by:

$$X_{i\_scale} = \frac{X_i - \mu_i}{\sigma_i} \quad (7)$$

where,

X_i = Feature *i*

μ_i = Mean of Feature *i*

σ_i = Standard Deviation of Feature *i*

7. RESULTS AND DISCUSSION

To validate the utility of the methodology proposed, Random Forest, SVM, and KNN Ml models have been considered for training and fivefold cross-validation. The feature vector is constructed from 46 features computed from 64 experimental conditions. In the beginning, to develop ML models, all features are needed for training. Afterward testing and fivefold cross-validation are carried out to assess the efficacy of our proposed procedure for fault identifications. To execute, fivefold cross-validation, the features vector is split into five equal-sized folds and then five iterations are performed. In the first stage, one fraction of five-fold is utilized for testing and the remaining four fractions are used for training. Similarly, in the second stage, two parts are used for testing, and the remaining three parts are used for training. The process will continue, till five-fold and finally, the results of the average classification are obtained. To identify the relevant features, we performed a feature ranking with LASSO (Least Absolute Shrinkage and Selection Operator) and the classified features are listed in Table 2. These 46 features are ordered accordingly the modified feature vector is adopted for fault identification. Table 3, shows the fault identification accuracy achieved after applying training, testing, and five-fold cross-validations. As observed from Table 3, 100 % training and testing accuracy was achieved with Random Forest and 93.8 % maximum accuracy with five-fold cross-validation. SVM identifies all faults with a maximum of 100 % training accuracy, and 78.90% testing accuracy with twenty-three ranked features. Similarly,81.3% five-fold cross-validation accuracy at the fourth feature is reported from SVM. Another classifier, KNN identifies faults with a maximum 100 % training accuracy, with twenty-nine ranked features and 94.70% testing,92.2% five-fold cross-validation accuracy with twenty-sixth and twenty-ninth features. Thus, it can be seen from Table 3 that compared to the other two classifiers, Random Forest offers the best identification accuracy with training, testing, and five-fold cross-validation. When Random forest is applied along with LASSO techniques, bearing faults are identified at less computational cost and with optimum accuracy. For multi-fault conditions, classification accuracy depicts the overall performance of the developed model. To know whether all fault conditions are predicted equally well, the confusion matrix plays a vital role. Table 4 shows the confusion matrix which allows us to visualize the individual class-wise prediction of the performance of the machine learning algorithm. In our study, we have included the confusion matrix which is obtained after performing training and cross-validation on ranked feature vectors with different classifiers. In the confusion matrix, columns and rows represent the actual and predicted classes. The diagonal matrix depicts the cases, where predicted cases are equal to the actual cases.

The Sum of all values of the diagonal matrix gives the predicted accuracy. While observing the confusion matrix obtained from SVM, all cases are correctly predicted when training of classifier was done whereas 52 cases are correctly predicted and 12 cases are incorrectly predicted. With Random Forest ML model, again all cases with all four conditions were predicted correctly from training, whereas 60 cases are predicted correctly and only 4 cases are predicted incorrectly with five-fold cross-validation. Similarly, with the KNN classifier, again all cases and all fault conditions predicted correctly with training and 59 cases predicted correctly and 5 cases are incorrectly predicted respectively. It can be seen that Random forest gives maximum accuracy when cross-validation accuracy is considered followed by SVM and ANN respectively. Further, out of all three fault conditions, the ORD fault condition is predicted correctly as compared to the other two fault conditions and at the same time, the normal condition of bearing is predicted with 100 % accuracy.

Table 2. Lasso Features

Sr. No.	Feature Name	Sr. No.	Feature Name
1	Maximum Probability	24	Sum Entropy
2	Information Measure of Correlation 2	25	Peak to RMS Ratio
3	Energy	26	Crest Factor
4	Covariance	27	Signal to Noise and Distortion Ratio
5	Median	28	Norm Entropy
6	Variance	29	Inverse Difference Normalized
7	Mean	30	Kurtosis
8	Homogeneity	31	Sum Average
9	Inverse Difference	32	Difference Variance
10	Information Measure of Correlation 1	33	Sum of Squares Variance
11	Standard Deviation	34	Contrast
12	Root Mean Square	35	Inverse Difference Moment Normalized
13	Mode	36	Auto Correlation
14	Correlation	37	Sure Entropy
15	L Factor	38	Shape Factor
16	Minimum Value in Signal	39	Sum Variance
17	Maximum Value in Signal	40	Maximum to Minimum Difference
18	Difference Entropy	41	Log Energy Entropy
19	Entropy	42	Form Factor
20	Root Sum of Squares	43	Cluster Shade
21	Skewness	44	Cluster Prominence
22	Shannon Entropy	45	Correlation Coefficient
23	Dissimilarity	46	Threshold Entropy

Table 3. Training, Testing, and 5-Fold Cross Validation Accuracies

Classifier / Rank	SVM			Random forest			KNN		
	Training	Testing	5-fold	Training	Testing	5-fold	Training	Testing	5-fold
1	56.3	42.10	43.8	92.2	42.10	40.6	90.6	42.10	37.5
2	92.2	63.20	64.1	**100**	36.80	53.1	**100**	52.60	67.2
3	92.2	63.20	71.9	100	47.40	60.9	100	57.90	75
4	**100**	73.70	**81.3**	100	84.20	89.1	100	78.90	84.4
5	100	52.60	65.6	100	63.20	79.7	100	52.60	73.4
6	100	68.40	65.6	100	100	85.9	100	78.90	75
7	100	57.90	56.3	100	73.70	85.9	100	78.90	71.9
8	100	52.60	60.9	100	84.20	85.9	100	68.40	73.4
9	100	63.20	53.1	100	**94.70**	84.4	100	63.20	75
10	100	57.90	53.1	100	84.20	85.9	100	63.20	65.6
11	100	57.90	67.2	100	84.20	84.4	100	68.40	75
12	100	52.60	68.8	100	100	82.8	100	78.90	82.8
13	100	68.40	64.1	100	84.20	79.7	100	73.70	70.3
14	100	63.20	68.8	100	84.20	87.5	100	78.90	84.4
15	100	68.40	59.4	100	100	89.1	100	68.40	84.4
16	100	57.90	64.1	100	84.20	82.8	100	68.40	81.3
17	100	57.90	57.8	100	94.70	84.4	100	84.20	84.4
18	100	73.70	62.5	100	89.50	90.6	100	78.90	82.8
19	100	68.40	67.2	100	78.90	85.9	100	73.70	84.4
20	100	68.40	64.1	100	100	90.6	100	89.50	73.4
21	100	56.30	57.8	100	100	85.9	100	75	84.4
22	100	68.40	60.9	100	84.20	90.6	100	84.20	81.3
23	100	**78.90**	64.1	100	84.20	**93.8**	100	89.50	84.4
24	100	68.40	64.1	100	89.50	85.9	100	89.50	81.3
25	100	52.60	64.1	100	78.90	87.5	100	73.70	87.5
26	100	63.20	64.1	100	84.20	92.2	100	**94.70**	81.3
27	100	57.90	54.7	100	89.50	76.6	100	78.90	89.1
28	100	47.40	56.3	100	100	85.9	100	94.70	84.4
29	100	47.40	56.3	100	84.20	92.2	100	94.70	**92.2**
30	100	47.40	57.8	100	84.20	89.1	100	89.50	85.9
31	100	47.40	57.8	100	84.20	87.5	100	94.70	81.3
32	100	57.90	53.1	100	94.70	89.1	100	84.20	81.3
33	100	68.40	53.1	100	84.20	81.3	100	84.20	89.1
34	100	52.60	59.4	100	78.90	84.4	100	84.20	82.8
35	100	68.40	57.8	100	78.90	85.9	100	94.70	85.9
36	100	47.40	56.3	100	84.20	90.6	100	84.20	85.9
37	100	52.60	54.7	100	94.70	89.1	100	89.50	84.4
38	100	47	56.3	100	78.90	90.6	100	74	79.7
39	100	57.90	56.3	100	89.50	89.1	100	78.90	85.9
40	100	57.90	53.1	100	94.70	84.4	100	84.20	85.9
41	100	52.60	56.3	100	89.50	92.2	100	78.90	82.8
42	100	47.40	53.1	100	89.50	89.1	100	73.70	81.3
43	100	52.60	54.7	100	84.20	90.6	100	94.70	81.3
44	100	52.60	54.7	100	73.70	82.8	100	84.20	87.5
45	100	52.60	57.8	100	78.90	92.2	100	73.70	79.7
46	100	63.20	53.1	100	84.20	85.9	100	89.50	82.8

Table 4. Confusion Matrix

	BD	NB	IRD	ORD
BD	16	0	0	0
NB	0	4	0	0
IRD	0	0	16	0
ORD	0	0	0	28

(a) Training accuracy (SVM)

	BD	NB	IRD	ORD
BD	10	0	1	5
NB	0	4	0	0
IRD	1	0	11	4
ORD	0	0	1	27

(b) Fivefold accuracy (SVM)

	BD	NB	IRD	ORD
BD	16	0	0	0
NB	0	4	0	0
IRD	0	0	16	0
ORD	0	0	0	28

(c) Training accuracy (SVM)

	BD	NB	IRD	ORD
BD	15	0	0	1
NB	0	4	0	0
IRD	1	0	13	2
ORD	0	0	0	28

(d) Fivefold accuracy (Random Forest)

	BD	NB	IRD	ORD
BD	16	0	0	0
NB	0	4	0	0
IRD	0	0	16	0
ORD	0	0	0	28

(e) Training accuracy (KNN)

	BD	NB	IRD	ORD
BD	15	0	0	1
NB	0	4	0	0
IRD	0	0	13	3
ORD	1	0	0	27

(f) Fivefold accuracy (KNN)

8. CONCLUSION

In this paper, bearing fault diagnosis is performed with the application of FWHT, LASSO, and ML models. From FWHT coefficients and GLCM features, a hybrid feature vector is initially constructed. with different bearing fault conditions. Important and meaningful features are identified from LASSO based feature ranking technique. Training, Testing, and cross-validation accuracies are calculated using SVM, Random forest, and KNN models. The results indicate that the FWHTranked features identify various bearing faults with good accuracy and can be further extended to other signal processing methods and with the ranked features for different rotating machinery components like turbines, gears rotors, pumps, etc.

ACKNOWLEDGEMENT

The authors would like to recognize the support of PDEU, Gandhinagar, and thank The Case Western Reserve University bearing vibration data sets, which is utilized in our investigation, to develop the methodology.

REFERENCES

[1] Lou, X. and Loparo, K.A.: Bearing fault diagnosis based on wavelet transform and fuzzy inference. Mechanical systems and signal processing, Vol.18, No. 53, pp.1077-1095, 2004.

[2] Prieto, M.D., Cirrincione, G., Espinosa, A.G., Ortega, J.A. and Henao, H.: Bearing fault detection by a novel condition-monitoring scheme based on statistical-time features and neural networks. IEEE Transactions on Industrial Electronics, Vol. 60, No. 8, pp.3398-3407, 2012.

[3] Jiang, F., Zhu, Z., Li, W., Chen, G. and Zhou, G.: Robust condition monitoring and fault diagnosis of rolling element bearings using improved EEMD and statistical features. Measurement Science and Technology, Vol.25, No.2, pp.025003, 2013.

[4] Sokolov, A.N., Pyatnitsky, I.A. and Alabugin, S.K.: Applying methods of machine learning in the task of intrusion detection based on the analysis of industrial process state and ICS networking. FME Transactions, Vol. 47, No. 4, pp.782-789, 2019.

[5] Dave, V., Singh S. and Vakharia, V.:Diagnosis of bearing faults using multi fusion signal processing techniques and mutual information. Indian Journal of Engineering & Materials Sciences, Vol. 27, pp.878-888, 2020.

[6] Vakharia, V., Gupta, V.K. and Kankar, P.K.: Nonlinear dynamic analysis of ball bearings due to varying number of balls and centrifugal force. Mechanisms and Machine Science, Vol. 21, pp.1103–1113, 2015.

[7] Kankar, P.K., Sharma, S.C. and Harsha, S.P.: Vibration based performance prediction of ball bearings caused by localized defects. Nonlinear Dynamics, Vol.69, No. 3, pp.847-875, 2012.

[8] Kankar, P.K., Sharma, S.C. and Harsha, S.P.: Rolling element bearing fault diagnosis using wavelet transform. Neurocomputing, Vol.74,No.10, pp.1638-1645, 2011.

[9] Gao, H., Liang, L., Chen, X. and Xu, G.: Feature extraction and recognition for rolling element bearing fault utilizing short-time Fourier transform and non-negative matrix factorization. Chinese Journal of Mechanical Engineering, Vol. 28, No. 1, pp.96-105, 2015.

[10] Rai, V.K. and Mohanty, A.R.: Bearing fault diagnosis using FFT of intrinsic mode functions in Hilbert–Huang transform. Mechanical Systems and Signal Processing, Vol. 21, No. 6, pp.2607-2615, 2007.

[11] Lei, Y., Lin, J., He, Z. and Zuo, M.J.: A review on empirical mode decomposition in fault diagnosis of rotating machinery. Mechanical systems and signal processing, Vol. 35, No. 1, pp.108-126, 2013.

[12] Daubechies, I.: The wavelet transform, time-frequency localization and signal analysis. IEEE transactions on information theory, Vol. 36, No. 5, pp.961-1005, 1990.

[13] Huang, N.E., Shen, Z., Long, S.R., Wu, M.C., Shih, H.H., Zheng, Q., Yen, N.C., Tung, C.C. and Liu, H.H.: The empirical mode decomposition and the Hilbert spectrum for nonlinear and non-stationary time series analysis. Proceedings of the Royal Society of London. Mathematical, physical and engineering sciences, Vol. 454, No. 1971, pp.903-995, 1998.

[14] Abodena, O. and Agoyi, M.:Colour Image Blind Watermarking Scheme Based on Fast Walsh Hadamard Transform and Heisenberg Decomposition. Studies in Informatics and Control, Vol. 27, No. 3, pp.339-348, 2018.

[15] Gao, Q., Tang, H., Xiang, J., Zhong, Y., Ye, S. and Pang, J.: A Walsh transform-based Teager energy operator demodulation method to detect faults in axial piston pumps. Measurement, Vol. 134, pp.293-306, 2019.

[16] Xiang, X., Zhou, J., Li, C., Li, Q. and Luo, Z.: Fault diagnosis based on Walsh transform and rough sets. Mechanical Systems and Signal Processing, Volume 23, No. 4, pp. 1313-1326, 2009.

[17] Zhao, M., Tang, B. and Tan, Q.: Fault diagnosis of rolling element bearing based on S transform and gray level co-occurrence matrix. Measurement Science and Technology, Vol. 26, No. 8, p.085008, 2015.

[18] Haralick, R.M., Shanmugam, K. and Dinstein, I.H.:Textural features for image classification. IEEE Transactions on systems, man, and cybernetics, Vol. 6, pp.610-621, 1973.

[19] Kaplan, K., Kaya, Y., Kuncan, M., Mi□naz, M.R. and Ertunç, H.M.: An improved feature extraction method using texture analysis with LBP for bearing fault diagnosis. Applied Soft Computing, Vol. 87, pp.106019, 2020.

[20] Niu, L., Qian, M., Yang, W., Meng, L., Xiao, Y., Wong, K.K., Abbott, D., Liu, X. and Zheng, H.: Surface roughness detection of arteries via texture analysis of ultrasound images for early diagnosis of atherosclerosis. PloS one, Vol. 8, No. 10, pp.76880, 2013.

[21] Eleyan, A. and Demirel, H.: Co-occurrence matrix and its statistical features as a new approach for face recognition. Turkish Journal of Electrical Engineering & Computer Sciences, Vol. 19, No. 1, pp.97-107, 2011.

[22] Subasi, A. and Gursoy, M.I.: EEG signal classification using PCA, ICA, LDA and support vector machines. Expert systems with applications, Vol. 37, No. 12, pp. 8659-8666, 2010.

[23] Gao, C.C. and Hui, X.W.: GLCM-based texture feature extraction. Computer Systems &Applications, Vol. 19, No. 6, pp.195-198, 2010.

[24] Lu, C., Wang, Y., Ragulskis, M. and Cheng, Y.: Fault diagnosis for rotating machinery: A method based on image processing. PloS one, Vol. 11, No. 10, pp.e0164111, 2016.

[25] Yang, P. and Yang, G.: Feature extraction using dual-tree complex wavelet transform and gray-level co-occurrence matrix. Neurocomputing, Vol. 197, pp.212-220, 2016.

[26] Vinay, V.; Kumar, G.V.; Kumar, K.P: Application of chi square feature ranking technique and random forestclassifier for fault classification of bearing faults. In Proceedings of the 22th International Congress on Soundand Vibration, Florence, Italy, 12–16 July 2015.

[27] Xiao, D., Qin, C., Yu, H., Huang, Y. and Liu, C.: Unsupervised deep representation learning for motor fault diagnosis by mutual information maximization. Journal of Intelligent Manufacturing, Vol. 32, No. 2, pp.377-391, 2021.

[28] Vakharia, V., Gupta, V.K. and Kankar, P.K.:A comparison of feature ranking techniques for fault diagnosis of ball bearing. Soft Computing, Vol. 20, No. 4, pp.1601-1619, 2016.

[29] Xu, Y., Wu, Z., Chanussot, J. Wei, Z.: Joint recon–struction and anomaly detection from compressive hyperspectral images using Mahalanobis distance-regularized tensor RPCA. IEEE Transactions on Geoscience and Remote Sensing, Vol. 56, No. 5, pp. 2919-2930, 2018.

[30] Fino, Algazi.: Unified Matrix Treatment of the Fast Walsh-Hadamard Transform, IEEE Trans. Comput., Vol. C–25, No. 11, pp. 1142–1146, 1976.

[31] Patel, D., Thakker, H., Kiran, M. B., Vakharia, V.: Surface Roughness Prediction of Machined Components Using Gray Level Co-occurrence Matrix and Bagging Tree, FME Transactions, Vol.48, pp. 468-475, 2020

[32] Punithavathy, K., Poobal, S. and Ramya, M.M.: Performance evaluation of machine learning techniques in lung cancer classification from PET/CT images. FME Transactions, Vol.47, No. 3, pp.418-423, 2019.

[33] Patel, D., Vakharia, V., Kiran, M.B..: Texture Classification of Machined Surfaces Using Image Processing and Machine Learning Techniques., FME Transactions, Vol.47, pp.865-872, 2019.

[34] Adeniyi, D.A., Wei, Z. and Yongquan, Y.: Automated web usage data mining and recommendation system using K-Nearest Neighbor (KNN) classification method. Applied Computing and Informatics, Vol. 12, No. 1, pp.90-108, 2016.

[35] Moosavian, A., Ahmadi, H., Tabatabaeefar, A. and Khazaee, M.:Comparison of two classifiers; K-nearest neighbor and artificial neural network, for fault diagnosis on a main engine journal-bearing. Shock and Vibration, Vol. 20, No. 2, pp. 263-272, 2013.

[36] Breiman, L.: Random forests. Machine learning, Vol. 45, No. 1, pp. 5-32, 2001.

[37] Radivojević, D.S., Mirkov, N.S., Maletić, S.: Human activity recognition based on machine learning classification of smartwatch accelerometer dataset. FME Transactions, Vol.49, pp. 235-232, 2021.

[38] Xie, Z. and Xu, Y.: Sparse group L-ASSO based uncertain feature selection. International Journal of Machine Learning and Cybernetics, Vol. 5, No. 2, pp.201-210, 2014.

[39] Zhang, T.:Multi-stage convex relaxation for feature selection. Bernoulli, Vol. 19, No. 5B, pp.2277-2293, 2013.

[40] Gupta, P., Pradhan, M.K.: Fault detection analysis in rolling element bearing: A review. Materials Today: Proceedings, Vol. 4, No. 2, pp.2085-2094, 2017.

[41] Loparo K, https://csegroups.case.edu/bearingdata–center/ pages/download-data-file 2021.

NOMENCLATURE

F_{IR}	Inner Race Frequency
F_{OR}	Outer Race Frequency
F_{BALL}	Ball Frequency
F_{Cage}	Cage Frequency
x_i	I^{th} Feature
μ_i	Mean of Feature i
σ_i	Standard Deviation of Feature i

ИДЕНТИФИКАЦИЈА ГРЕШАКА У КУГЛИЧНИМ ЛЕЖАЈЕВИМА ПРИМЕНОМ БРЗЕ ВОЛШ АДАМАРД ТРАНСФОРМАЦИЈЕ, LASSO ИЗБОРА КАРАКТЕРИСТИКА И КЛАСИФИКАЦИЈОМ НАСУМИЧНЕ ШУМЕ

В. Дејв, Х. Такер, В. Вакхарија

Да би се открило стање исправности машине, анализа временске фреквенције је ефикасан алат када су сигнали нестационарне природе. У циљу идентификације грешке у лежајевима, разни истражи–вачи су предложили бројне технике. Међутим, мало истраживања се фокусирало на екстракцију карак–теристика текстуре засноване на обради слике за идентификацију грешака. Слика временске фрек–венције садржи много осетљивих информација о грешкама у вези са условима лежаја, које се могу издвојити у облику карактеристика. Стога је у овом документу предложена методологија заснована на временско-фреквенцијском спектрограму брзе Волш Адамардове трансформације (ФВХТ), матрици ко-појављивања сивог нивоа (ГЛЦМ) и техникама машинског учења. Конструише се вектор обележја који се састоји од једнодимензионалних и дво-димензионалних обележја екстрахованих из коефи–цијената Фаст Волш Адамард трансформације. Да би се идентификовали услови квара, примењује се рангирање карактеристика засновано на LASSO-у да би се одредиле одговарајуће карактеристике. Коначно, класификатори као што су машина за подршку векторима (МПВ), случајна шума и К-најближи суседи (КНС) се процењују за идентифи–кацију грешака у лежајевима. Обука, тестирање, петострука унакрсна валидација изведена на вектору карактеристика фузије. Добијени резултати показују да су рангиране карактеристике фузије ефикасне за дијагнозу кварова на лежајевима са добром тачношћу.